



Synthesis and characterization of nano magnetic wheat straw for lead adsorption

Zeinab Azizi Haghighat, Elham Ameri*

Department of Chemical Engineering, Shahreza Branch, Islamic Azad University, P.O. Box 311-86145, Shahreza, Iran, Tel. +98 321 3292242; Fax: +98 265 2423898; email: azizi.zeinab66@yahoo.com (Z. Azizi Haghighat), Tel. +98 31 53292508; Fax: +98 265 2423898; emails: ameri@iaush.ac.ir, amerielham@yahoo.com (E. Ameri)

Received 28 November 2014; Accepted 13 March 2015

ABSTRACT

In this study, an attempt was made for the first time to remove Pb(II) ions from aqueous solutions using magnetic wheat straw (MWS). MWS was synthesized using *in situ* co-precipitation method and characterized by BET, SEM, TEM, X-ray diffraction, Fourier transform infrared, and vibrating sample magnetometer methods. The biosorption characteristics of Pb(II) ions onto the wheat straw (WS) and MWS were studied with respect to some effective parameters, including solution pH, initial Pb(II) concentration, and dose of adsorbent. The initial solution pH and contact time for MWS were optimized to be 5.0 and 30 min, respectively. The equilibrium process was satisfactorily described by the Langmuir isotherm model with maximum sorption capacities of 50.76 and 41.15 mg g⁻¹ for MWS and WS, respectively. Kinetic studies for MWS indicated that both pseudo-first-order and pseudo-second-order kinetic models were able to describe the process with correlation coefficients of 0.978 and 0.9997, respectively.

Keywords: Magnetic wheat straw; Lead; Biosorption; Fe₃O₄ nano-particles

1. Introduction

Rapid industrialization has led to enhanced disposal of heavy metals into the environment. Environmentalists are anxious about the presence of heavy metals because of their toxic effects on human health and the environment. Lead is a toxic heavy metal released into the environment by applications such as ceramics, finishing tools, plastics, cathode ray tubes, solders, pieces of lead flashing, and other minor products as well as steel and cable reclamation.

Lead is a particularly harmful metal since once it enters the human body, it is diffused throughout quickly, leaving dangerous effects. For example, it can harm red blood cells and limit their ability to carry

oxygen to the organs. It can also disturb the kidneys, hearing, and the nervous system [1]. So it is quite clear that the determination of lead ions in water is necessary. Accordingly, some methods such as solid phase extraction have been applied for the selective determination of Pb(II) in water [2,3].

The conventional wastewater treatment methods used for lead and other heavy metals include reverse osmosis, electro dialysis, chemical precipitation, solvent extraction, filtration, ion exchange, phytoremediation, electroflotation, chemical oxidation or reduction, and coagulation. However, the applicability of the mentioned methods is often limited due to several disadvantages such as incomplete metal removal, high capital and operational costs, low selectivity, high reagent and energy requirements, fouling and

*Corresponding author.

instability of the membrane, and generation of toxic sludge or other waste products which are difficult to remove [4].

Biosorption has been shown to be a promising alternative method for the removal of heavy metals in wastewaters due to its high selectivity, easy handling, lower operating costs, and high efficiency [5]. Different agricultural wastes, viz. rice straw, soybean hulls, sugarcane bagasse, peanut shells, and walnut shells in their natural form, are good candidates for the removal of lead [6]. Moreover, the ability of modified soda lignin extracted from oil palm empty fruit bunches in removing lead(II) ions from aqueous solutions has been explored [7]. Waste tea leaves, flowers of *Humulus pulus*, petioler felt-seath of palm, and the agro-waste of black gram husk were investigated for the elimination of lead. It was found that the efficiency of these materials ranged from 70 to 98% [8–11]. The maximum adsorption of 94% for Pb(II) ions was obtained under the optimum condition using sawdust and neem bark [12]. Calcium-treated sargassum and rose petals pretreated with NaOH have also been employed for the significant removal of lead [13,14]. High efficiency for the removal of lead and other metal ions has been reported using activated carbon prepared from agricultural waste [15,16]. On the other hand, Singha and Das investigated the removal of lead ions from aqueous solutions and industrial effluents using natural biosorbents [17]. Using *Pinus sylvestries* led to 85–90% removal efficiency, but the results showed that modification did not improve the removal efficiency for lead [18]. Gundogdu et al. also investigated the biosorption potential of pine (*Pinus brutia* Ten) bark in a batch system for the removal of Pb(II) ions from aqueous solutions [19]. The adsorption capacity of rice husk ash for Pb(II) ions in terms of monolayer adsorption was reported to be 91.74 mg g^{-1} by Naiya et al. [20]. Naiya et al. also used clarified sludge and activated alumina for the removal of Pb(II) from aqueous solutions [21,22]. Recently, Chen et al. used a new low-cost adsorbent, fallen *Cinnamomum camphora* leaves for effective removal of Pb(II) from aqueous solutions [23]. In general, most studies have shown that lead biosorption by employing agricultural waste materials is effective, and extensive works have been reported for the removal of lead employing agricultural waste materials. On the other hand, as an agricultural waste, wheat straw (WS) has a high annual yield. However, most of the WS is usually burnt for heating or left directly to be decomposed. These treatments can not only discard natural resources, but also cause environmental pollutions. Hence, it is essential to make the best use of WS. It should also be noted that WS has a

vascular bundle structure affording some additional surface for chemical modifications. It has complicated components containing lignin, hemicellulose, cellulose, pectin, protein, and fatty acids [24]. The WS is plentiful in hydroxyl groups, which can offer chemical reaction sites and adsorb iron ions to grow Fe_3O_4 crystals. In this work, we used the agricultural waste WS as a template, grew Fe_3O_4 nano-particles on its surface, and then studied its potential application in lead biosorption.

The aims of this investigation were: (a) synthesis of magnetic wheat straw (MWS) by co-precipitation method and its characterization using SEM, TEM, X-ray diffraction (XRD), VSM, BET, and Fourier transform infrared (FTIR), (b) comparative batch adsorption study of the two adsorbents (WS and MWS) for Pb(II) with respect to various experimental parameters, and (c) comparative isotherm and kinetic studies.

2. Experimental

2.1. Materials

WS was collected from a local industry (Shiraz) and washed thoroughly with distilled water to remove any dirt. It was then dried in an oven at 65°C until it reached a constant weight, fed to a mixer and grinder, and ground. Finally, it was sieved for a particle size of $0.125\text{--}0.595 \times 10^{-3} \text{ m}$. Iron(II) sulfate heptahydrate ($\text{FeSO}_4 \cdot 7\text{H}_2\text{O}$), iron(III) chloride hexahydrate ($\text{FeCl}_3 \cdot 6\text{H}_2\text{O}$), and ammonia solution ($\text{NH}_3 \cdot \text{H}_2\text{O}$, 25%) were prepared from Merck (Darmstadt, Germany) and used for Fe_3O_4 synthesis. $\text{Pb}(\text{NO}_3)_2$ (from Merck) was used to obtain the solutions of Pb(II) ions. All chemicals, which were of analytical reagent grade, were purchased from Merck.

2.2. Synthesis of $\text{Fe}_3\text{O}_4/\text{WS}$

As a classical method, *in situ* co-precipitation was used to synthesize $\text{Fe}_3\text{O}_4/\text{WS}$ composites. The chemical reaction of Fe_3O_4 formation can be represented by the following equation:



In this work, about 0.5 g of WS fragments and a certain amount of $\text{NH}_3 \cdot \text{H}_2\text{O}$ (25%) were added to a 0.050-L mixed solution of FeSO_4 and FeCl_3 (the molar ratio of Fe^{3+} to Fe^{2+} was 2/1) under an inert gas. The temperature was raised and kept at 70°C for 4 h. After that, the $\text{Fe}_3\text{O}_4/\text{WS}$ composite was washed several times by deionized water and separated by a magnet;

finally, it was dried in vacuum at 50°C for 24 h. The magnetic nanoparticles were coded as MNP. The total iron ion concentration in the reaction mixture was 0.1 mol L⁻¹. The required amount of NH₃·H₂O (25%) added to the reaction mixture was 0.002 L.

2.3. Characterization methods

Scanning of WS and MWS was done using a field emission scanning electron microscope (FE SEM, HITACHI CHIS-4160). The average size and structure phases of the adsorbents were analyzed by XRD (D8 ADVANCE, Bruker). Infrared absorption spectroscopy (IR) spectra of adsorbents were monitored by FTIR spectroscopy using the KBr Pellet technique. The BET (Brunauer, Emmett, and Teller) surface areas for both adsorbents were measured using Smart Sorbs 92 surface area analyzer. TEM image of MWS was achieved by a transmission electron microscope (Philips CM30 FEI TECNAI G2 microscope operating at 250 kV). The magnetic properties of MWS were studied using a vibrating sample magnetometer (VSM, Lake Shore 7307) at room temperature in an applied magnetic field ranging from -10,000 G to 10,000 G.

2.4. Biosorption experiments

A stock solution including 1,000 mg L⁻¹ Pb(II) ions was prepared by dissolving a proper amount of Pb(NO₃)₂ in deionized water and subsequently diluted to the required concentrations closely prior to its use. The biosorption of Pb(II) ions onto the adsorbents was studied by the batch technique. The method employed for this purpose was as follows: the required amount of adsorbents was equilibrated with 0.025 L of aqueous solution of adsorbate (Pb(NO₃)₂) at different concentrations ranging from 10 to 1,000 mg L⁻¹ in different glass bottles on a shaker (Edmund Buhler, GmbH). According to the results obtained from some preliminary experiments, they were performed at the stirring speed of 240 rpm, using WS with the size of 149–125 × 10⁻⁶ m. The experiments were carried out at ambient temperature and different pH values varying from 2 to 6 in a shaking thermostat. The initial pH of the adsorbate solution was adjusted by adding enough amounts of diluted HNO₃ or NaOH solutions. The progress of biosorption was monitored at different time intervals until saturation was achieved. After the completion of predetermined time intervals, the content of one bottle was separated by high-speed centrifugation at 4,000 rpm and WS was removed by filtration through 0.45-μm nitrocellulose membrane (Sartorius Stedim Biotech., GmbH), while MWS was

removed magnetically from the aqueous solutions. Finally, the concentration of Pb(II) ions in the filtrate was determined by a flame atomic absorption spectrophotometer (FAAS) (A Analyst 300 Perkin Elmer, USA). All experiments were conducted in triplicate. The equilibrium adsorption capacity, Q_e , of Pb(II) aqueous was calculated using the mass balance according to the following equation:

$$Q_e = \frac{V(C_o - C_e)}{m} \quad (2)$$

where V is the sample volume (L), m is the mass of adsorbent (g), C_o represents the initial concentration of Pb(II) in the solution (mg L⁻¹), and C_e denotes the equilibrium concentration of Pb(II) in the solution (mg L⁻¹). For time-dependent data, C substitutes C_e and Q replaces Q_e in Eq. (2).

3. Results and discussion

3.1. Characterization of MWS

The nitrogen adsorption–desorption isotherm of WS and MWS was obtained and the data are represented in Table 1. TEM image with the surface morphology of MWS adsorbent was achieved, and the average diameter of MWS was found as shown in Table 1.

Scanning electron micrographs of WS and MWS are shown in Fig. 1(a) and (b), respectively. Fig. 1(a) shows that the parent WS material has insoluble cell walls with fibrous contents that could facilitate the adsorption of metals according to its irregular surface. Fig. 1(b) indicates that the WS was completely covered with iron oxide and all iron oxide particles were aggregated to make a spherical structure.

Fig. 2 depicts XRD patterns of the synthesized materials and WS. For MWS and MNP, the peaks located at $2\theta = 30.3^\circ, 35.6^\circ, 43.3^\circ, 57.15^\circ,$ and 62.9° were characteristic of Fe₃O₄. These peaks were consistent with the database in JCPDS file (PCPDFWIN v.2.02, PDF No. 85-1436), showing that the WS binding had no effect on the phase change of Fe₃O₄ in the composite. Also, the diffraction peaks at $2\theta = 17.1^\circ$ and 24.7° referred to the cellulose I crystalline form in both WS and MWS, which could be attributed to natural cellulose [24]. The average particle size of MWS was calculated to be 4.63 nm, using the standard Debye–Scherrer equation:

$$d = \frac{k\lambda}{\beta \cos \theta} \quad (3)$$

Table 1

Surface area and porosity of WS and MWS from N₂ adsorption analysis and average diameter of MNP on MWS from TEM analysis

Adsorbents	S_{BET} (m ² g ⁻¹)	V_{pore} (ml g ⁻¹)	d_{pore} (nm)	Average diameter of MNP on sorbent (nm)
WS	3.373	0.049	3.086	–
MWS	23.56	8.32	3.056	5.64

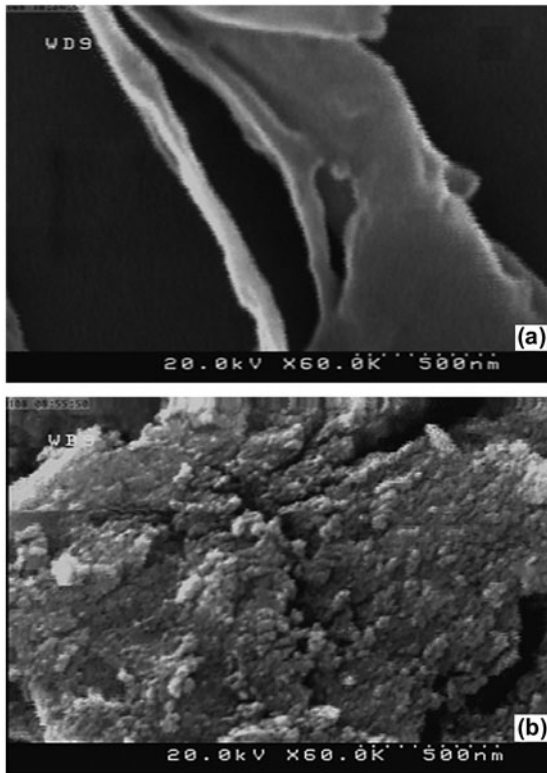


Fig. 1. SEM images of (a) WS and (b) MWS.

where d refers to the particles size, k represents the Debye–Scherrer constant (0.89), λ is the X-ray wavelength (0.15406 nm), and β and θ are the full width at half maximum and the Bragg angle, respectively.

The FT-IR technique is known as the main tool to recognize some characteristic functional groups acting as adsorbents for the removal of metal ions and dye. Infrared spectra of WS, MNP, and MWS are presented in Fig. 3.

As shown in Fig. 3, the spectra illustrated a number of absorption peaks signifying the complex nature of the material. The broad peaks around 3,346.28 cm⁻¹ were attributed to the bonded hydroxyl groups on the surface of the parent WS. This band was assigned to the vibration of the silanol group, hydroxyl group linked to cellulose and lignin, and the water adsorbed onto the parent adsorbent. The

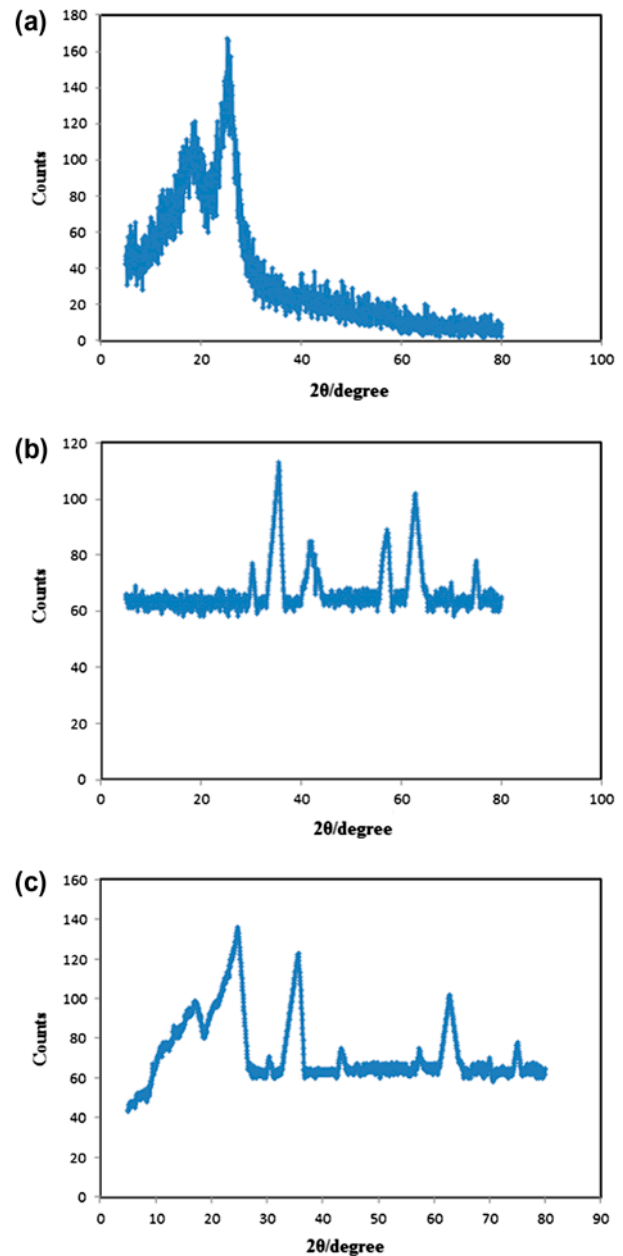


Fig. 2. XRD patterns of (a) WS, (b) MNP, and (c) MWS.

peaks which appeared at 2,920.48 and 1,375.30 cm⁻¹ were due to the stretching vibration and the bending vibration of the C–H bond in the methyl group,

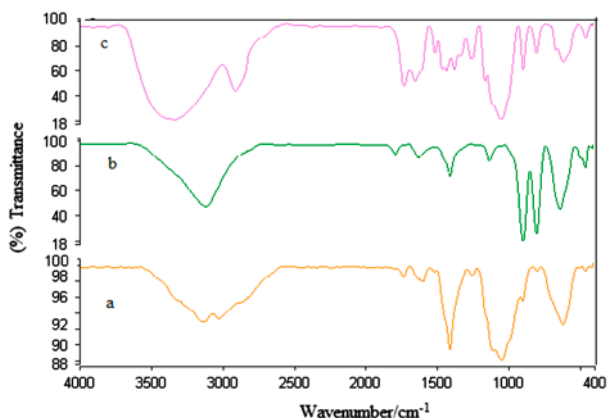


Fig. 3. FT-IR spectra of (a) WS, (b) MNP, and (c) MWS.

respectively. The absorption peaks around $1,733.86$ and $1,658.38\text{ cm}^{-1}$ were indicative of the existence of the carbonyl group stretching from aldehydes and ketones [25]. The peak located at $1,427\text{ cm}^{-1}$ was characteristic of the stretch vibration of C–O from the hydroxyl group. The strong C–O band located at $1,054\text{ cm}^{-1}$ also indicated the lignin structure of WS. The peak near $1,253.06\text{ cm}^{-1}$ was also attributed to the stretch vibration of C–O in phenols.

Spectroscopic analysis exhibited in Fig. 3 reveals the successful binding of MNP onto the WS surface. A comparison between the two spectra of MWS and MNP in Fig. 3 showed that the characteristic peak of MNP at $3,120\text{ cm}^{-1}$ (OH stretch) and 638.68 cm^{-1} (Fe–O) underwent a specific shift in MWS spectra to $3,141.23\text{ cm}^{-1}$ (OH) and 615.51 cm^{-1} (Fe–O), which could be assigned to the interaction of the hydroxyl groups and metal oxide on MNP during MWS formation. Moreover, a comparison of WS and MWS spectra showed the shifting, disappearance, and appearance of peaks. The significant band shifting from $3,346.28$ to $3,141.23\text{ cm}^{-1}$ (OH stretching), $2,920.48$ to $3,040.39\text{ cm}^{-1}$ (–CH stretching), $1,733.86$ to $1,737.78\text{ cm}^{-1}$ (C=O stretching), $1,429.12$ to $1,404.83\text{ cm}^{-1}$ (C–OH), and $1,051.62$ to $1,043.04\text{ cm}^{-1}$ (C–O–C stretching) indicated the successful binding of WS onto MNP to form MWS.

Zero point charge (pH_{pzc}) is the main property specifying the electrical neutrality of the biosorbent at a particular value of pH. The pH_{pzc} values of WS and MWS were found to be 2.1 and 2.6, respectively. This indicated that MWS was positively charged at $\text{pH} < 2.6$.

The magnetic hysteresis loops at 298 K of MWS are exhibited in Fig. 4. MWS typically demonstrates the superparamagnetic behavior, thereby indicating that the magnetic material can respond to an applied magnetic field without any permanent magnetization,

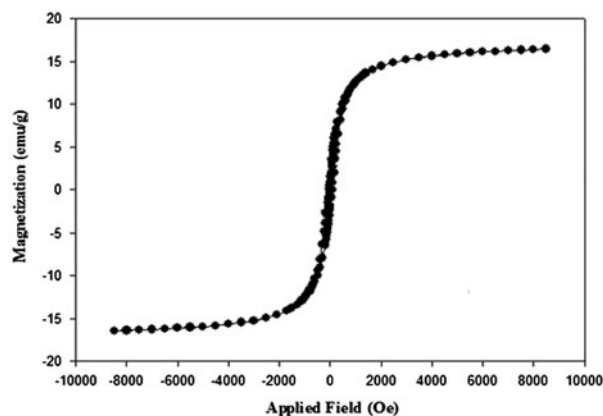


Fig. 4. Magnetic hysteresis loops of MWS at 298 K.

with the loop area being zero. The saturated magnetization for MWS was found to be 5.65 emu g^{-1} with regard to Fe_3O_4 content. Superparamagnetic materials can be simply separated from the solution with the aid of an external magnetic field. According to this characteristic, the MWS can be very advantageous if used as the material for adsorption processes.

3.2. Equilibrium contact time

In order to achieve the equilibrium time for maximum metal ions uptake onto WS and MWS, a study on contact time was carried out. Experiments were carried out for different contact times with a fixed adsorbent dose of 4 g L^{-1} for the solution, initial concentration of 100 mg L^{-1} , pH of 5.0, and shaking rate of 240 rpm. A graph of removal percentage vs. time (Fig. 5) represents the rapid adsorption of metal ions during the first 5 min; thereafter, the adsorption of Pb(II) was slowly improved and became almost constant at 70 min in the case of WS, and 30 min for MWS. Finally, after reaching the saturation values of 85.37 and 71.2%, a smooth graph was achieved using MWS and WS, respectively.

The reduction in the extraction rate of metal ions with time could be due to the aggregation of metal ions around the adsorbent particles. This aggregation could obstruct the migration of adsorbate as the adsorption sites were filled up and the resistance to the dispersion of metal ions in the adsorbents was enhanced. In addition, the occupation of the remaining active sites could be difficult according to the repulsive forces between the lead ions on the adsorbent and the remaining lead ions in the aqueous solution.

Moreover, the higher adsorption efficiency for lead ions onto MWS could be attributed to the available functional groups on the adsorbent surface and the

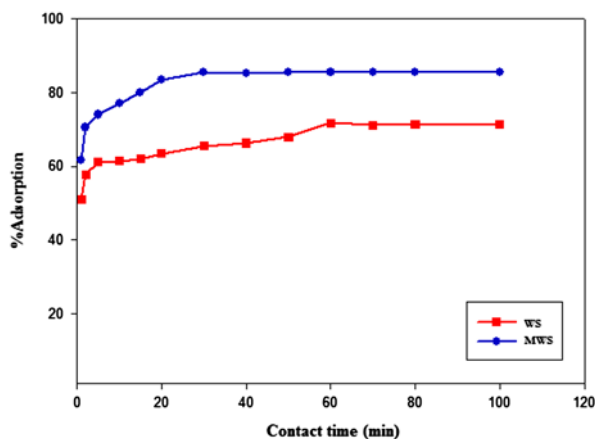


Fig. 5. Effect of contact time on the adsorption of lead(II) onto WS and MWS (initial lead(II) concentration = 100 mg L^{-1} , pH 5, adsorbent dose = 4 g L^{-1} , and shaking rate = 240 rpm).

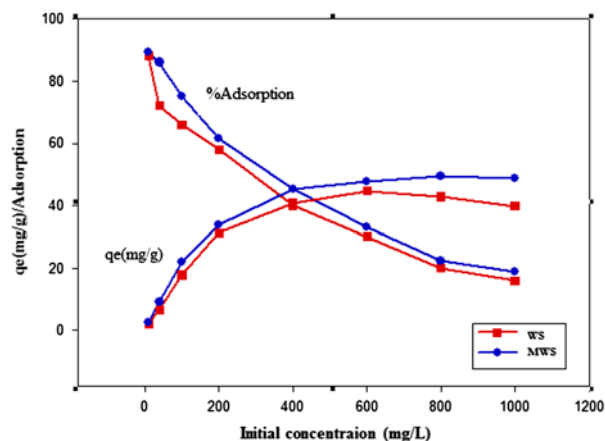


Fig. 6. Effect of the initial concentration of lead(II) ion adsorption (adsorbent dose = 4 g L^{-1} , pH 5, shaking rate = 240 rpm, and contact time = 30 min for MWS and 70 min for WS).

higher surface area of MWS. According to the values reported for the surface area of WS and MWS, it was found that better adsorption capability led to higher adsorption efficiency for lead ions onto MWS. However, surface areas of both WS and MWS were less than $25 \text{ m}^2/\text{g}$, and higher adsorption efficiency for lead ions onto MWS could be due to this reason. In other words, a faster adsorption rate for MWS could be attributed to the external surface adsorption created by nonporous nano adsorbent, which was different from the microporous adsorption process obtained by the WS [26]. Since nearly all adsorption sites of MWS were present on their exterior, it was easy for the adsorbate to access these active sites, thereby causing the fast approach to equilibrium. This result can be promising due to the advantage of the economic viability as equilibrium time is known to play the main role in designing a wastewater treatment plant.

3.3. Effect of concentration of adsorbate

To determine the effect of initial metal ion concentration on the adsorption process, the initial concentration of Pb(II) was changed from 10 to $1,000 \text{ mg L}^{-1}$. Batch adsorption experiments were performed at pH 5, with an adsorbent dose of 4 g L^{-1} and the shaking rate of 240 rpm. It is evident from Fig. 6 that the efficiency of Pb(II) removal was affected by the initial metal ion concentration at contact durations of 30 and 70 min using MWS and WS, respectively.

At low metal ion concentrations, metal ion adsorption included higher energy sites. Since the metal ion concentration was enhanced, the higher energy sites

were saturated and adsorption was started on lower energy sites, thereby causing reductions in the adsorption efficiency. As shown in Fig. 6, at the lowest concentration of lead (10 mg L^{-1}), the removal percentages were 89.3 and 88% for MWS and WS, respectively. Further enhancement in the lead concentration to $1,000 \text{ mg L}^{-1}$ led to a decrease in the removal percentages to 18.9 and 16% for MWS and WS, respectively.

3.4. Effect of pH

To investigate the effect of pH, the adsorption of Pb(II) was studied with an adsorbent dose of 32 g L^{-1} , initial ion concentration of 400 mg L^{-1} , and shaking rate of 240 rpm. The results are shown in Fig. 7.

The pH range was selected to be 2–6 in order to avoid metal hydroxides, which had been estimated to happen at pH >6.5 for $\text{Pb}(\text{OH})_2$ [27]. Fig. 7 demonstrates that maximum adsorption capacity happened at pH 5. Similar values of optimum pH for the adsorption of Pb(II) have been reported in the literature using the spent grain [28], *Pinus sylvestris* [18], and crop milling waste [11] as the biosorbent.

As it can be seen in Fig. 7, the change in pH affected the adsorption process. The reduction in the adsorption capacity of WS and MWS at lower pHs could be due to the competition faced by Pb(II) ions with H^+ ions adsorbed onto the binding sites of the cells, which were responsible for lead adsorption [14].

On the other hand, the H^+ ion concentration could react with the functional groups located on the active sites on the adsorption surface. Generally, adsorption

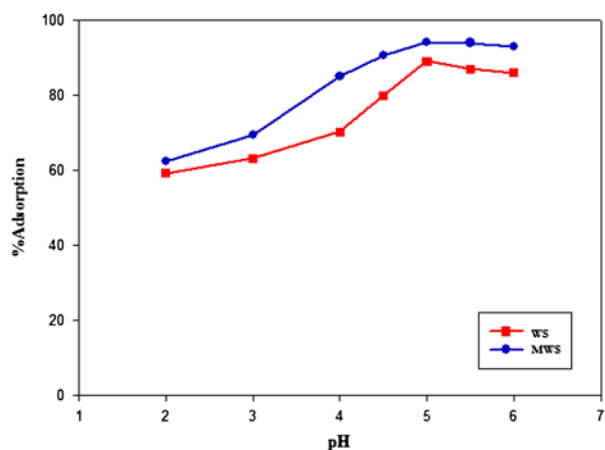


Fig. 7. Effect of the solution pH on lead(II) ion adsorption (initial lead(II) concentration = 400 mg L^{-1} , pH 5, adsorbent dose = 32 g L^{-1} , shaking rate = 240 rpm, and contact time = 30 min for MWS and 70 min for WS).

of cations was favored at $\text{pH} > \text{pH}_{\text{PZC}}$, whereas the pH_{PZC} values were 2.6 and 2.1 for MWS and WS, respectively.

Moreover, when pH was enhanced, there was a decrease in positive surface charge (since the deprotonation of the functional groups of WS, especially hydroxyl, could occur) that resulted in a lower electrostatic repulsion between the positively charged lead ion and the surface of WS favoring adsorption.

A study in the literature [29] on Pb(II) speciation has illustrated that the dominant species are $\text{Pb}(\text{OH})_2$ at $\text{pH} > 6.0$ and Pb^{2+} and $\text{Pb}(\text{OH})^+$ at $\text{pH} < 6.0$. Upon further increase in $\text{pH} > 6$, adsorption was reduced,

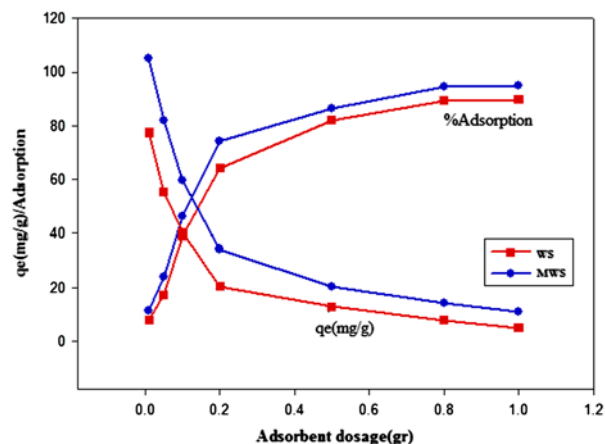


Fig. 8. Effect of adsorbent dosage on lead(II) adsorption (initial lead(II) concentration = 400 mg L^{-1} , pH 5, shaking rate = 240 rpm, and contact time = 30 min for MWS and 70 min for WS).

but the total lead removal was improved according to adsorption and the formation of lead hydroxide, which was precipitated [30,31]. The optimized value of pH for adsorption was found to be 5, where $\text{Pb}(\text{OH})_2$ precipitation did not happen. Thereafter, the pH value of 5 was chosen for adsorption experiments based on the maximum adsorption capacity.

3.5. Effect of the adsorbent dosage

Fig. 8 shows the adsorption of lead(II) ions by WS and MWS at different extents of the adsorbent (0.01–1.0 g), initial concentration of 400 mg L^{-1} lead solution, and the shaking rate of 240 rpm. When the adsorbent extent was enhanced from 0.01 to 1.0 g, the removal percentage was generally improved, but the amount adsorbed per unit mass of adsorbent was found to be

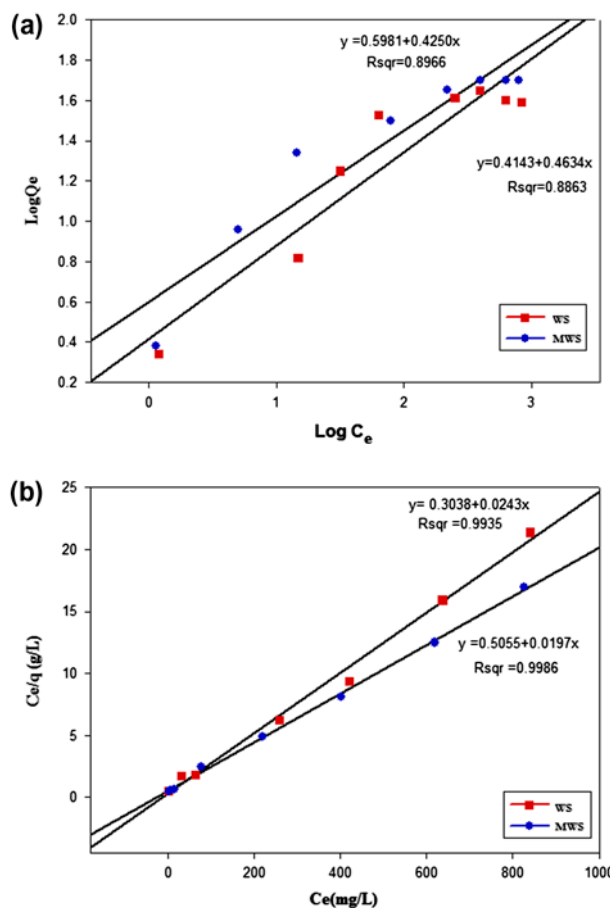


Fig. 9. (a) Freundlich isotherm plot for the removal of Pb(II) on WS and MWS and (b) Langmuir isotherm plot for the removal of Pb(II) on WS and MWS (adsorbent dose = 4 g L^{-1} , pH 5, shaking rate = 240 rpm, contact time = 30 min for MWS and 70 min for WS, ambient temperature).

Table 2

Langmuir and Freundlich isotherm constants for Pb(II) biosorption on WS and MWS (adsorbent dose = 4 g L⁻¹, pH 5, shaking rate = 240 rpm, contact time = 30 min for MWS, 70 min for WS, ambient temperature)

Langmuir isotherm	q_m (mg g ⁻¹)	b (L mg ⁻¹)	R^2
WS	41.15	0.0800	0.994
MWS	50.76	0.0389	0.999
Freundlich isotherm	K_F (mg ^{1-1/n} L ^{1/n} g ⁻¹)	n (unitless)	R^2
WS	1.513	2.16	0.886
MWS	1.819	2.35	0.897

diminished considerably. Removal percentage reached the maximum (approximately, 90% for WS and 95% for MWS) at around 0.8 g and then remained almost constant.

The rise in the removal percentage or reduction in unit adsorption with the increase in the dose of adsorbent was based on the enhancement in the active sites on the adsorbent, thus making the penetration of the lead ions to the adsorption sites easier. Moreover, when the adsorbent extent was up to 0.8 g, the enhancement in lead(II) adsorption was not considerable. This could be attributed to the formation of adsorbent agglomerates which decreased the available surface area and blocked some adsorption sites. Similar results have been reported by others [32].

3.6. Adsorption isotherms

The aim of the adsorption isotherms is to correlate the adsorbate concentration in the solution and the adsorbed extent of the metal ions at the adsorbate–adsorbent interface. Freundlich and Langmuir isotherm models are widely applied by environmentalists to optimize a design of the adsorption system. In the present study, the adsorption of Pb(II) ions onto WS and MWS adsorbents was investigated, and the applicability of the mentioned isotherms was examined. The Langmuir model assumes that the sorption of metal ions happens on a homogenous surface by monolayer adsorption with no interaction between the adsorbed ions. The Langmuir and Freundlich models can be expressed as shown in Eqs. (4) and (5), respectively:

$$Q_e = \frac{Q_{\max} b C_e}{(1 + b C_e)} \quad (4)$$

where Q_e is the extent of metal adsorbed onto the biosorbent (mg g⁻¹), C_e is the equilibrium concentration of metal adsorbed in the solution (mg L⁻¹), Q_{\max} represents the maximum adsorption capacity or the

theoretical monolayer saturation capacity, and b is the Langmuir equilibrium constant [33].

$$Q_e = K_F \cdot C_e^{1/n} \quad (5)$$

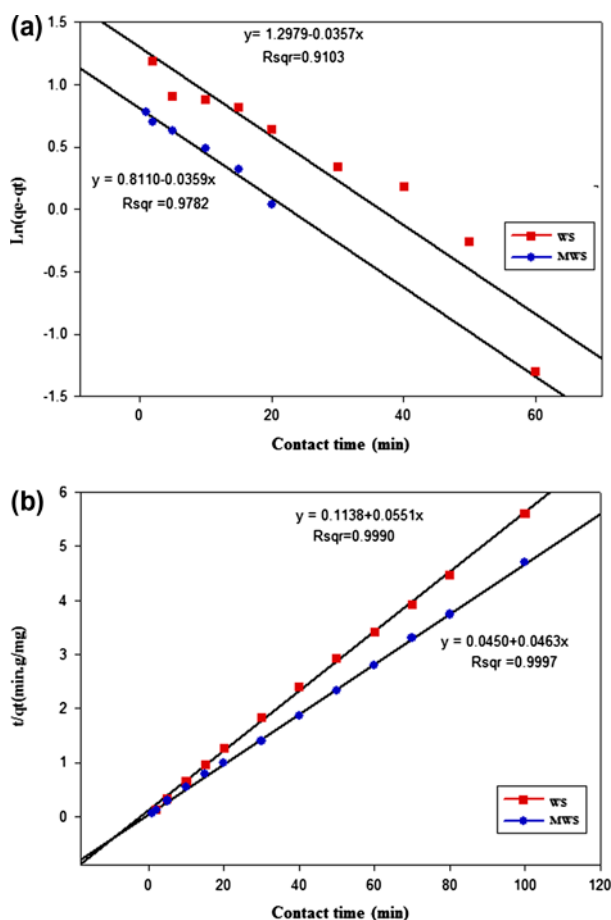


Fig. 10. (a) Pseudo-first-order kinetics of Pb(II) onto WS and MWS and (b) pseudo-second-order kinetics Pb(II) onto WS and MWS (initial lead(II) concentration = 100 mg L⁻¹, pH 5, adsorbent dose = 4 g L⁻¹, shaking rate = 240 rpm, ambient temperature).

Table 3

Characteristic parameters of the kinetic pseudo-first-order and pseudo-second-order models and coefficients of determination (initial lead(II) concentration = 100 mg L⁻¹, pH 5, adsorbent dose = 4 g L⁻¹, shaking rate = 240 rpm, ambient temperature)

Adsorbent	Pseudo-first order		Pseudo-second order	
	R ²	k × 10 ³ (min ⁻¹)	R ²	k × 10 ³ (mg ⁻¹ g min ⁻¹)
WS	0.910	35.7	0.9990	26.7
MWS	0.978	35.9	0.9997	47.6

For the Freundlich model, K_F (mg^{1-1/n} L^{1/n} g⁻¹) is the constant associated with the adsorption capacity of the adsorbent, n (dimensionless) is the exponent associated with adsorption intensity [34]. The experimental data were fitted to both Langmuir and Freundlich isotherms (Fig. 9). The isotherm constants in Eqs. (4) and (5), as well as the regression coefficients (R^2), are given in Table 2.

1/ n value for Pb(II) lies between 0 and 1, thereby indicating favorable adsorption. It was found that the Langmuir model was best fitted to the experimental data with the values of the coefficient of determination, R^2 , being 0.994 for WS and 0.999 for MWS as illustrated in Fig. 9. This shows that the used adsorbents would provide monolayer and homogeneous adsorption of the lead ions.

3.7. Biosorption kinetics

The rate at which sorption happens is of great importance when designing batch sorption experiments. Accordingly, it is essential to find biosorption kinetics containing the search for the best model that can well characterize the experimental data.

The pseudo-first-order equation widely applied to predict metal sorption experiments has the following form:

$$\frac{dQ}{dt} = k_1(Q_e - Q_t) \quad (6)$$

where Q_t (mg g⁻¹) is the amount of metal ions biosorbed at time t , Q_e is the amount of metal ions biosorbed at equilibrium (mg g⁻¹), and k_1 is the rate constant of the biosorption (min⁻¹). After definite integration by considering the conditions $Q_t = 0$ at $t = 0$ and $Q_t = Q_t$ at $t = t$, the equation is rewritten as the following equation:

$$\ln(Q_e - Q_t) = \ln Q_e - k_1 t \quad (7)$$

Straight line in the graph of $\ln(Q_e - Q_t)$ vs. t shows the applicability of this kinetic model. Q_e and

k_1 can be estimated from the intercept and the slope of the plot, respectively. The linear plots of $\ln(Q_e - Q_t)$ vs. t for the pseudo-first-order kinetic model using WS and MWS are presented in Fig. 10(a).

The pseudo-second-order rate equation has been widely applied to explain metal ions and organic compound sorption onto diverse sorbents.

$$\frac{dQ}{dt} = k_2(Q_e - Q_t)^2 \quad (8)$$

where Q_t and Q_e (mg g⁻¹) are the extents of biosorption at time t (min) and at equilibrium, respectively; k_2 (g mg⁻¹ min⁻¹) is the rate constant of the second-order equation. After definite integration using the conditions $Q_t = 0$ at $t = 0$ and $Q_t = Q_t$ at $t = t$, the equation is rewritten as the following equation:

$$\frac{t}{Q_t} = \frac{1}{k_2 \cdot Q_e^2} + \frac{t}{Q_e} \quad (9)$$

The plot of t/Q_t vs. t should give a straight line if second-order kinetics is appropriate, and Q_e and k_2 can be estimated from the slope and the intercept of the plot, respectively. The linear plots of t/Q_t vs. t for the pseudo-second-order kinetic model using WS and MWS are presented in Fig. 10(b).

The values of correlation coefficients (Table 3) for both adsorbents showed a better fit of the pseudo-second-order model with the experimental data with respect to the Lagergren first-order model; so, one can conclude that the rate-limiting step is of chemisorption nature. In this regard, the results of kinetic analysis for *Saccharomyces cerevisiae* biomass showed that the biosorption process of Pb(II) ions followed pseudo-second-order kinetics [35].

4. Conclusions

The efficiency of magnetic nanoparticles impregnated onto WS waste in removing lead(II) ions from aqueous solutions was studied. Characterization studies showed various physico-chemical properties of

MWS which were favorable for metal binding. The adsorbents revealed good adsorption capacity for lead ions. The adsorption capability of the nanocomposite was higher than that of WS. The results showed that the biosorption process for WS and MWS was highly pH dependent. The optimum pH value was found to be 5. The higher percentage removal of lead ions could be achieved at lower initial lead concentrations. Adsorption data were well fitted by the Langmuir isotherm for MWS and WS. The kinetics of adsorption (for WS and MWS) followed both pseudo-first-order and pseudo-second-order kinetics. The results of this investigation suggest that the developed MWS shows not only high adsorption efficiency and faster kinetics but also other benefits like easy recovery, absence of secondary pollutants, cost-effectiveness, and environmental-friendliness. Therefore, it can be recommended for wastewater treatments and control of environmental pollution.

References

- [1] S. Zhu, H. Hou, Y. Xue, Retracted: Kinetic and isothermal studies of lead ion adsorption onto bentonite, *Appl. Clay Sci.* 40 (2008) 171–178.
- [2] M. Ghaedi, M. Montazerzohori, M. Soylak, Solid phase extraction method for selective determination of Pb(II) in water samples using 4-(4-methoxybenzylidene-imine) thiophenole, *J. Hazard. Mater.* 142 (2007) 368–373.
- [3] M. Soylak, I. Narin, M.D.A. Bezerra, S.L.C. Ferreira, Factorial design in the optimization of preconcentration procedure for lead determination by FAAS, *Talanta* 65 (2005) 895–899.
- [4] G. Zhang, R. Qu, C. Sun, C. Ji, H. Chen, C. Wang, Y. Niu, Adsorption for metal ions of chitosan coated cotton fiber, *J. Appl. Polym. Sci.* 110 (2008) 2321–2327.
- [5] B. Benguella, H. Benaissa, Cadmium removal from aqueous solutions by chitin: Kinetic and equilibrium studies, *Water Res.* 36 (2002) 2463–2474.
- [6] M.M. Johns, W.E. Marshall, C.A. Toles, Agricultural by products as granular activated carbons for adsorbing dissolved metals and organics, *J. Chem. Technol. Biotechnol.* 71 (1998) 131–140.
- [7] M.N. Ibrahim, W.S. Ngah, M.S. Norliyana, W.R. Daud, M. Rafatullah, O. Sulaiman, R. Hashim, A novel agricultural waste adsorbent for the removal of lead(II) ions from aqueous solutions, *J. Hazard. Mater.* 182 (2010) 377–385.
- [8] S.S. Ahluwalia, D. Goyal, Removal of heavy metals by waste tea leaves from aqueous solution, *Eng. Life Sci.* 5 (2005) 158–162.
- [9] J. Gardea-Torresdey, M. Hejazi, K. Tiemann, J.G. Parsons, M. Duarte-Gardea, J. Henning, Use of hop (*Humulus lupulus*) agricultural by-products for the reduction of aqueous lead(II) environmental health hazards, *J. Hazard. Mater.* 91 (2002) 95–112.
- [10] M. Iqbal, A. Saeed, N. Akhtar, Petiolar felt-sheath of palm: A new biosorbent for the removal of heavy metals from contaminated water, *Bioresour. Technol.* 81 (2002) 151–153.
- [11] A. Saeed, M. Iqbal, M.W. Akhtar, Removal and recovery of lead(II) from single and multimetal (Cd, Cu, Ni, Zn) solutions by crop milling waste (black gram husk), *J. Hazard. Mater.* 117 (2005) 65–73.
- [12] T.K. Naiya, A.K. Bhattacharya, S.K. Das, Adsorption of Pb(II) by sawdust and neem bark from aqueous solutions, *Environ. Prog.* 27 (2008) 313–328.
- [13] O. Karnitz Jr., L.V.A. Gurgel, J.C.P. de Melo, V.R. Botaro, T.M.S. Melo, R.P. de Freitas Gil, L.F. Gil, Adsorption of heavy metal ion from aqueous single metal solution by chemically modified sugarcane bagasse, *Bioresour. Technol.* 98 (2007) 1291–1297.
- [14] M.H. Nasir, R. Nadeem, K. Akhtar, M.A. Hanif, A.M. Khalid, Efficacy of modified distillation sludge of rose (*Rosa centifolia*) petals for lead(II) and zinc(II) removal from aqueous solutions, *J. Hazard. Mater.* 147 (2007) 1006–1014.
- [15] M. Aliabadi, I. Khazaei, H. Fakhraee, M.T.H. Mousavian, Hexavalent chromium removal from aqueous solutions by using low-cost biological wastes: Equilibrium and kinetic studies, *Int. J. Environ. Sci. Technol.* 9 (2013) 319–326.
- [16] K. Wilson, H. Yang, C.W. Seo, W.E. Marshall, Select metal adsorption by activated carbon made from peanut shells, *Bioresour. Technol.* 97 (2006) 2266–2270.
- [17] B. Singha, S.K. Das, Removal of Pb(II) ions from aqueous solution and industrial effluent using natural biosorbents, *Environ. Sci. Pollut. Res.* 19 (2012) 2212–2226.
- [18] V.C. Taty-Costodes, H. Fauduet, C. Porte, A. Delacroix, Removal of Cd(II) and Pb(II) ions, from aqueous solutions, by adsorption onto sawdust of *Pinus sylvestris*, *J. Hazard. Mater. B* 105 (2003) 121–142.
- [19] A. Gundogdu, D. Ozdes, C. Duran, V.N. Bulut, M. Soylak, H.B. Senturk, Biosorption of Pb(II) ions from aqueous solution by pine bark (*Pinus brutia* Ten.), *Chem. Eng. J.* 153 (2009) 62–69.
- [20] T.K. Naiya, A.K. Bhattacharya, S. Mandal, S.K. Das, The sorption of lead(II) ions on rice husk ash, *J. Hazard. Mater.* 163 (2009) 1254–1264.
- [21] T.K. Naiya, A.K. Bhattacharya, S.K. Das, Clarified sludge (basic oxygen furnace sludge)—An adsorbent for removal of Pb(II) from aqueous solutions—Kinetics, thermodynamics and desorption studies, *J. Hazard. Mater.* 170 (2009) 252–262.
- [22] T.K. Naiya, A.K. Bhattacharya, S.K. Das, Adsorption of Cd(II) and Pb(II) from aqueous solutions on activated alumina, *J. Colloid Interface Sci.* 333 (2009) 14–26.
- [23] H. Chen, J. Zhao, G. Dai, J. Wu, H. Yan, Adsorption characteristics of Pb(II) from aqueous solution onto a natural biosorbent, fallen *Cinnamomum camphora* leaves, *Desalination* 262 (2010) 174–182.
- [24] R. Liu, H. Yu, Y. Huang, Structure and morphology of cellulose in wheat straw, *Cellulose* 12 (2005) 25–34.
- [25] C.R. Tarley, M.A. Arruda, Biosorption of heavy metals using rice milling by-products. Characterisation and application for removal of metals from aqueous effluents, *Chemosphere* 54 (2004) 987–995.
- [26] N.N. Nassar, Rapid removal and recovery of Pb(II) from wastewater by magnetic nano-adsorbents, *J. Hazard. Mater.* 184 (2010) 538–546.

- [27] C.F. Baes, R.E. Mesmer, *The Hydrolysis of Cations*, Wiley, New York, NY, 1976.
- [28] K.S. Low, C.K. Lee, S.C. Liew, Sorption of cadmium and lead from aqueous solutions by spent grain, *Proc. Biochem.* 36 (2000) 59–64.
- [29] V. Gomez-Serrano, A. Macias-Garcia, A. Espinosa-Mansilla, C. Valenzuela-Calahorro, Adsorption of mercury, cadmium and lead from aqueous solution on heat-treated and sulphurized activated carbon, *Water Res.* 32 (1998) 1–4.
- [30] A. Aklil, M. Mouflih, S. Sebti, Removal of heavy metal ions from water by using calcined phosphate as a new adsorbent, *J. Hazard. Mater.* 112 (2004) 183–190.
- [31] N. Khalid, S. Rahman, S. Ahmad, Potential of sawdust for the decontamination of lead from aqueous media, *Sep. Sci. Technol.* 40 (2005) 2427–2443.
- [32] E. Cheraghi, E. Ameri, A. Moheb, Continuous biosorption of Cd(II) ions from aqueous solutions by sesame waste: Thermodynamics and fixed-bed column studies, *Desalin. Water Treat.* (2015) 1–14.
- [33] I. Langmuir, The adsorption of gases on plane surfaces of glass, mica and platinum, *J. Am. Chem. Soc.* 40 (1918) 1361–1403.
- [34] H.M.F. Freundlich, Uber die adsorption in losungen (Over the adsorption in solution), *Z. Phys. Chem. (J. Phys. Chem.)* 57 (1906) 385–470.
- [35] M. Ghaedi, G.R. Ghezelbash, F. Marahel, S. Ehsanipour, A. Najibi, M. Soylak, Equilibrium, thermodynamic, and kinetic studies on lead(II) biosorption from aqueous solution by *Saccharomyces cerevisiae* biomass, *Clean—Soil, Air, Water* 38 (2010) 877–885.